

# An Electronic Mach-Zehnder Interferometer

Yang Ji, Yunchul Chung, D. Sprinzak, M. Heiblum, D. Mahalu, and Hadas Shtrikman

Braun Center for Submicron Research, Department of Condensed Matter Physics, Weizmann Institute of Science, Rehovot 76100, Israel

(March 22, 2022)

*Double-slit* electron interferometers, fabricated in high mobility two-dimensional electron gas (2DEG), proved to be very powerful tools in studying coherent wave-like phenomena in mesoscopic systems [1–6]. However, they suffer from small fringe visibility due to the many channels in each slit and poor sensitivity to small currents due to their *open geometry* [3–5,7]. Moreover, the interferometers do not function in a high magnetic field, namely, in the quantum Hall effect (QHE) regime [8], since it destroys the symmetry between left and right slits. Here, we report on the fabrication and operation of a novel, single channel, two-path electron interferometer that functions in a high magnetic field. It is the first *electronic analog* of the well-known optical *Mach-Zehnder* (MZ) interferometer [9]. Based on single *edge state* and *closed geometry* transport in the QHE regime the interferometer is highly sensitive and exhibits very high visibility (62%). However, the interference pattern decays precipitously with increasing electron temperature or energy. While we do not understand the reason for the dephasing we show, via shot noise measurement, that it is not a decoherence process that results from inelastic scattering events.

Direct phase measurements of electrons, customarily done in double-slit interferometers [1–4], are difficult to perform under strong magnetic fields. Electrons are being diverted by the Lorentz force, perform chiral skipping orbits, and prefer one slit to the other - thus breaking the symmetry of the interferometer. At the extreme quantum limit, namely, in the QHE regime, the *skip-ping orbits* quantize to quasi-one-dimensional like states, named *chiral edge states*. We exploited the chiral motion of the electrons and constructed an electronic analog of the ubiquitous optical Mach-Zehnder (MZ) interferometer [9] (described schematically in Fig. 1a). A beam splitter **BS1** splits an incoming monochromatic light beam from source **S** into two beams, which, after reflection by mirrors **M1** and **M2**, recombine and interfere at **BS2** to result in two outgoing beams (collected by detectors **D1** and **D2**). When the phase along one of the paths varies both signals in **D1** and in **D2** oscillate out of phase, and since no photons are being lost the sum of both signals stays always equal to the input in **S**. In the electronic counterpart, depicted in Fig. 1b, *quantum point contacts* (QPC) function as beam splitters and *Ohmic contacts* serve as detectors. A QPC is formed in the 2DEG by depositing a split metallic gate on the surface of the semiconductor and biasing it negatively with respect to the 2DEG. The induced potential in the 2DEG creates a barrier under the gate bringing the two oppositely propagating edge currents to the small opening in the barrier, allowing thus backscattering. As shown schematically in Fig. 1b QPC1 splits the incoming edge current from **S** to two paths, a transmitted *inner path* and a reflected *outer path*, both later recombine and interfere in QPC2, to result with two edge currents (collected by **D1** and **D2**).

The actual device, seen in Fig. 1c, was fabricated in a high mobility 2DEG embedded in a GaAs-AlGaAs het-

erojunction. A ring-shaped mesa,  $3\mu\text{m}$  in width, was defined by plasma etching with Ohmic contacts (for **S**, **D1**, and **D2**) connected to the inner and outer edges of the ring. The inner contact, **D2**, and the two QPCs are connected to outside sources via air bridges that float above the mesa. A phase difference  $\varphi$  between the two paths is introduced via the Aharonov-Bohm (AB) effect [10,11],  $\varphi = 2\pi BA/\phi_0$ , with  $B$  the magnetic field,  $A$  the area enclosed by the two paths ( $\sim 45\mu\text{m}^2$ ), and  $\phi_0 = 4.14 \times 10^{-15}\text{Tm}^2$  the flux quantum. A few *modulation gates*, **MG**, are added above the outer path in order to tune the phase  $\varphi$  by changing the area  $A$ . We briefly review the operation of the interferometer. At filling factor 1 in the QHE regime a single chiral edge state carries the current. The interfering current, in turn, is proportional to the transmission probability from source to drain  $T_{SD}$ . Neglecting dephasing processes and having the transmission (reflection) amplitude  $t_i$  ( $r_i$ ) of the  $i^{\text{th}}$  QPC fulfilling  $|r_i|^2 + |t_i|^2 = 1$ , then [7]  $I_{D1} \propto T_{SD1} = |t_1 t_2 + r_1 r_2 e^{i\varphi}|^2 = |t_1 t_2|^2 + |r_1 r_2|^2 + 2|t_1 t_2 r_1 r_2| \cos\varphi$  and  $I_{D2} \propto T_{SD2} = |t_1 r_2 + r_1 t_2 e^{i\varphi}|^2 = |t_1 r_2|^2 + |r_1 t_2|^2 - 2|t_1 t_2 r_1 r_2| \cos\varphi$ . Note that ideally the two currents oscillate out of phase as function of  $\varphi$  while  $T_{SD1} + T_{SD2} = 1$ . The visibility of the oscillation is defined as:  $v = (I_{\text{max}} - I_{\text{min}})/(I_{\text{max}} + I_{\text{min}})$  and, for example, when QPC2 is tuned so that  $T_2 = 0.5$ , the visibility is  $v = 2\sqrt{T_1(1 - T_1)}$ .

Measurements were done at filling factor 1 (magnetic field  $\sim 5.5\text{T}$ ) and also at filling factor 2 with similar results. With a refrigerator temperature  $\sim 6\text{mK}$  the electron temperature was determined by measuring the equilibrium noise [12] to be  $\sim 20\text{mK}$ . High sensitivity measurement of the interference pattern was conducted at  $\sim 1.4\text{MHz}$  with a spectrum analyzer. Current at **D1** (or **D2**) was filtered and amplified in situ by LC circuit and a low noise home-made pre-amplifier, both placed near the sample and cooled to  $1.5\text{K}$ .

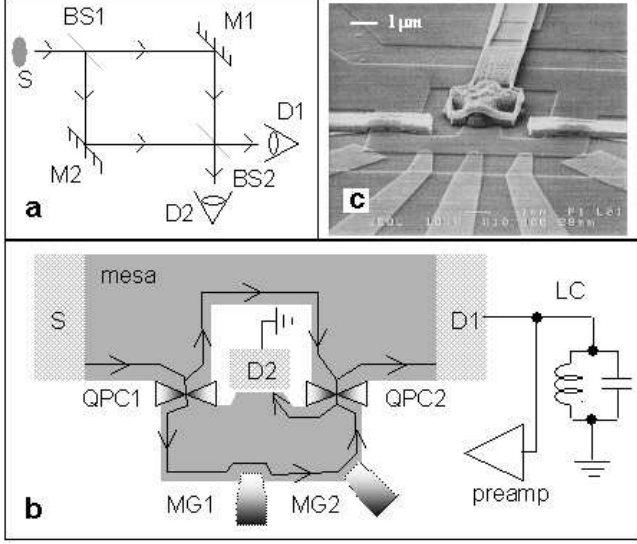


FIG. 1. The configuration and operation of an optical Mach-Zehnder interferometer and its actual realization with electrons. (a) Schematics of an optical Mach-Zehnder interferometer. **D1** and **D2** are detectors, **BS1** and **BS2** are beam splitters, and **M1** and **M2** are mirrors. With  $0(\pi)$  phase difference between the two paths, **D1** measures maximum (zero) signal and **D2** zero (maximum) signal. The sum of the signals in both detectors is constant and equals to the input signal. (b) Schematics of the electronic Mach-Zehnder interferometer and the measurement system. Edge states are formed in a high perpendicular magnetic field. The incoming edge state from **S** is split by **QPC1** (quantum point contact) to two paths, of which one moves along the inner edge and the other along the outer edge of the device. The two paths meet again at **QPC2**, interfere, and result in two complementary currents in **D1** and in **D2**. By changing the contours of the outer edge state and thus the enclosed area between the two paths, the modulation gates (**MG**) tune the phase difference between the two paths via the Aharonov-Bohm effect. A high signal-to-noise-ratio measurement of the current in **D1** is performed at 1.4MHz with a cold LC resonant circuit as a band pass filter followed by a cold, low noise, preamplifier. (c) SEM picture of the device. A centrally located small Ohmic contact ( $3 \times 3 \mu m^2$ ), serving as **D2**, is connected to the outside circuit by a long metallic air-bridge. Two smaller metallic air-bridges bring the voltage to the inner gates of **QPC1** and **QPC2** - both serve as beam splitters for edge states. The five metallic gates (at the lower part of the figure) are modulation gates (**MG**).

A standard lock-in technique, with a low-frequency signal (7Hz,  $10 \mu V$  RMS), gave similar results, however, the measurement lasted much longer and was prone to samples instability. Since at 5.5T each flux quantum occupies an area of some  $10^{-15} m^2$  (some 60,000 flux quanta thread the area **A**), a minute fluctuation in the superconducting magnets current or in the area would smear the interference signal. Two measurement methods were employed. The first relied on the unavoidable decay of

the short-circuited current that circulates in the superconducting magnet (being in the so called, *persistent current mode*). In this mode the magnetic field decays smoothly at a rate of  $\sim 0.12 mT/hour$  ( $\sim 1$  flux quantum every 50 minutes). The second was via scanning the voltage on a modulation gate at a rate much faster than the decay rate of the magnetic field, thus changing the area **A**, the enclosed flux, and consequently the AB phase.

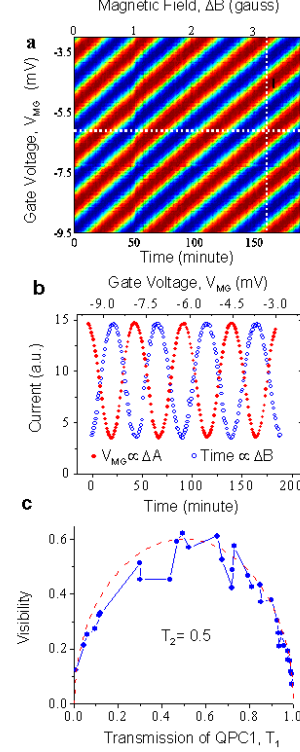


FIG. 2. Interference pattern of electrons in a Mach Zehnder interferometer and the dependence on transmission. (a) Two dimensional color plot of the current collected by **D1** as function of magnetic field and gate voltage at an electron temperature of  $\sim 20 mK$ . The magnet was set in its persistent current mode ( $B \sim 5.5 T$  at filling factor 1 in the bulk) with a decay rate of some  $0.12 mT/hour$ , hence time appears on the abscissa. The two QPCs were both set to transmission  $T_1 = T_2 = 0.5$ . Red (blue) stands for high (low) current. (b) The current collected by **D1** plotted as function of the voltage on a modulation gate (red plot) and as function of the magnetic field (blue plot) - along the cuts shown in a. The visibility of the interference is 0.62. (c) The visibility of the interference pattern as a function of the transmission probability  $T_1$  of **QPC1** when **QPC2** is set to  $T_2 = 0.5$ . Dashed line is a fit to the experimental data with visibility  $= 2\eta\sqrt{T_1(1-T_1)}$ . The normalization coefficient  $\eta=0.6$  accounts for possible decoherence and/or phase averaging.

We first test the ideality of the Ohmic contacts and the validity of the edge states picture. For both QPCs open a nearly ideal Hall plateau was observed in  $I_{D1}$  while no current was measured in **D2** ( $I_{D2}=0$ ). That

validated that current was confined to the outer edge with no backscattering across the  $3\mu\text{m}$  wide mesa. We then pinched off QPC1 or QPC2 and found again a Hall plateau in  $I_{D2}$  with zero current in **D1** ( $I_{D1} = 0$ ). This proved that the small Ohmic contact of **D2** was ideal and fully absorbed the current. Setting then both QPCs to  $T_1 = T_2 \sim 1/2$  and varying the magnetic field  $B$  (actually the time) or the area  $A$  (the voltage on a **MG**) lead to pronounced interference signal in **D1** (or in **D2**) with visibility as high as 0.62 (Fig. 2). Since the field decays linearly with time and the area (or electron density) vary proportional to the gate voltage changing these parameters leads to the diagonal straight color lines (of constant phase) seen in Fig. 2a. Figure 2b shows similar data taken along two cuts (the dotted lines shown in Fig. 2a) - one for constant  $B$  and one for constant  $A$ . The cleanliness of the interference pattern and the high visibility prove the nearly ideal nature of the interferometer.

In order to further verify the *two-path nature* of the interference the visibility was measured as function of  $T_1$  for a constant  $T_2 = 0.5$  (see Fig. 2c). It agrees well with the expected expression for the visibility  $v = 2\eta\sqrt{T_1(1-T_1)}$ , with  $\eta \sim 0.6$  a normalization factor that accounts for dephasing (either due to phase averaging in the energy window of the electrons or due to inelastic scattering processes). Moreover, the period of the oscillations, in time and in **MG** voltage, agrees well with one flux quantum being added (or subtracted) in the rings area. The time period is  $\sim 50\text{min}$ , which is the time needed for one flux quantum decay in the superconducting magnet, while the voltage period agrees approximately with that needed to deplete one electron (hence, one flux quantum for filling factor 1) under the **MG** gate.

While the visibility is very high it is still smaller than unity ( $v \sim 0.6$ ). An obvious reason is the finite energy spread of the electrons at the edge (due to their finite temperature) and the unavoidable dependence of the AB area on the energy (hence, the AB phase) - leading to phase averaging (*thermal smearing*). Indeed, the visibility was found to drop precipitously with increasing temperature or applied voltage at **S**, as seen in Fig. 3. In this example, a mere increase of the temperature to 100mK (some  $9\mu\text{eV}$ ) reduced the visibility from  $v \sim 0.53$  to  $v \sim 0.01$  (plotted in red in Fig. 3a). If indeed phase averaging is the cause for the dephasing, it could, in principle, be eliminated with monoenergetic electrons. A minute AC signal ( $\sim 0.5\mu\text{V}$ ) at 1.4MHz was added to a variable DC voltage  $V_{DC}$  and the synchronous AC part of the interfering signal was measured at 20mK. This signal leads to a *differential visibility*  $v_d$ , resulting only from the electrons in an energy window  $\sim 0.5\mu\text{eV}$  around an energy  $eV_{DC}$ . Surprisingly, as seen in Fig. 3a (plotted in blue), the energy dependent differential visibility at  $T=20\text{mK}$  is strikingly similar to the temperature dependent visibility with a relation between the scales  $eV_{DC} \sim 4k_B T$ . The visibility (in color scale)

is plotted as function of both  $T$  and  $V_{DC}$  in Fig. 3b. The clear symmetry across the diagonal suggests that the dephasing processes due to temperature and voltage are similar. Unfortunately this contradicts our previous assertion of phase averaging taking place in a wide window of energy and points at decoherence, induced by inelastic scattering events, as the main source of dephasing. In other words, for an increased temperature or for high energy monoenergetic electrons, empty states are being created allowing energy loss via scattering.

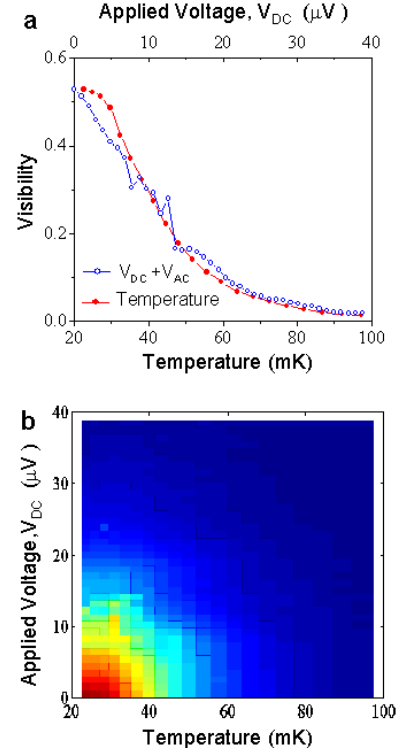


FIG. 3. The dependence of the visibility of the interference pattern on temperature and applied voltage. (a) Visibility as function of temperature at small excitation voltage for  $V_{DC} = 0$  (red plot), and as function of  $V_{DC}$  with a small AC voltage  $V_{AC}$  superimposed on it at electron temperature 20mK (blue plot). Both QPCs were set to  $T_1 = T_2 = 0.5$ . (b) A 2D color plot of the visibility as function of temperature and applied DC voltage. Red (blue) stands for high (low) visibility.

In order to test this hypothesis current shot noise was measured. Its spectral density, defined as the averaged square of the current fluctuations per unit of frequency,  $S = \langle (i^2) \rangle / \Delta f$ , and for stochastic partitioning at zero temperature  $S \propto eV_{DC}T_{SD}(1-T_{SD})$  [13]. Introducing a phenomenological parameter  $k$  that accounts for decoherence in the interferometer with  $T_1 = 1/2$  and  $T_{SD} = 0.5 + k\sqrt{T_2(1-T_2)\cos\varphi}$ , we find that for complete phase averaging or for a complete decoherence  $T_{SD} = 0$ . On the other hand shot noise in **D1** is

$S_{D1} \propto T_{SD1}(1 - T_{SD1}) = 1/4 - k^2 T_2(1 - T_2) \cos^2 \varphi$ , with  $S_{D1} = \text{const.}$  for  $k = 0$  but  $S_{D1} = 1/4 - k^2 T_2(1 - T_2)/2$  for complete phase averaging (resulting from an integration of  $\cos^2 \varphi$  in the range  $\varphi = 0 \dots 2\pi$ ). Hence, noise is expected to exhibit a parabolic dependence on  $T_2$  in a coherent system. Shot noise was measured (see Refs. 12 and 13 for details) with a relatively large  $V_{DC}$  applied at **S** so that interference signal was quenched (negligible visibility). The dependence of  $S$  on  $T_2$ , shown in Fig. 4, followed the above expression with  $k \sim 0.9$ , proving that indeed phase averaging is dominant while decoherence is negligibly small.

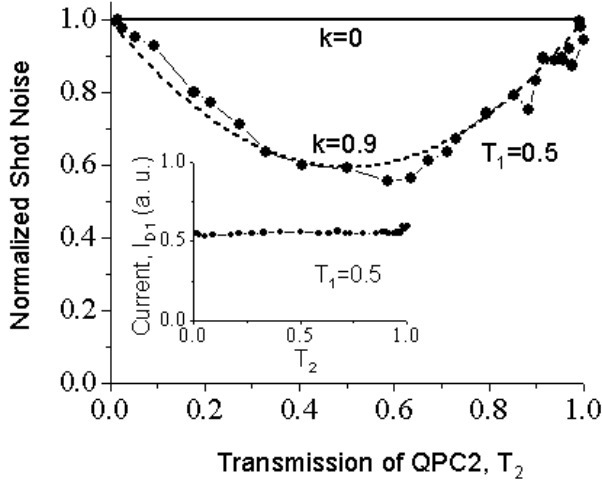


FIG. 4. Shot noise measurement (at filling factor 2) as function of  $T_2$  when the transmission of QPC1 was set to  $T_1 = 0.5$ . A  $30\mu\text{V}$  DC voltage (under which the AB interference pattern was quenched) was used to measure shot noise. The shot noise of the current collected by **D1** is shown by the black dots (normalized to a maximum), while the two solid lines are the expected noise for  $k = 0$  and  $k = 0.9$ , respectively, according to the simple model described in the text. The agreement with the simple model indicates that the electrons are coherent even at the DC voltage where the interference pattern fades away. Inset: the current at **D1** as function of  $T_2$  at  $V_{DC} = 30\mu\text{V}$ . As expected from the lack of the interference pattern, the current is independent of  $T_2$  (see text).

A single particle, namely, a non-interacting model would lead to the following dependences of the visibility on energy: for  $V = 0$  and finite  $T$ ,  $v \propto \beta T / \sinh(\beta T)$ , with  $\beta$  a constant; for finite  $V$  but  $T = 0$ ,  $v \propto \sin[(e/2\pi)V] / [(e/2\pi)V]$ , while the differential visibility at  $T = 0$  is expected to be voltage independent. Since the experimental results contradict these projections we propose (with no proof yet) two possible reasons for the dephasing. One might be due to low frequency noise (say,  $1/f$  type due to moving impurities), which might be induced by a higher current, leading to fluctuation in the area and consequently, phase smearing. The other could be related to the self consistent potential contour at the

edge. Since it depends on the local density of the electrons in the edge state [14], fluctuation in the density due to partitioning are expected to lead to fluctuation in the AB area enclosed by the two paths and hence to phase randomization. For example, for  $B \sim 5.5\text{T}$  a merely  $1\sim 2$  angstroms shift of the edge suffices to add one flux quantum into the enclosed area.

Our aim here was to present a novel and powerful electron interferometer, which might to be used as a powerful tool for future interferometry studies of electrons. One exciting possibility is the study of coherence and phase of fractionally charged quasiparticles in the fractional quantum Hall effect regime [15].

*Acknowledgements* We thank Y. Levinson for clarifying the issue of phase averaging and C. Kane for providing useful comments on the manuscript. The work was partly supported by the MINERVA Foundation, the Israeli Academy of Science, the German Israeli Project Cooperation (DIP), the German Israeli Foundation (GIF), and the EU QUACS network.

- 
- [1] Yacoby, A., Heiblum, M., Umansky, V., Shtrikman, H., Mahalu, D. Unexpected periodicity in an electronic double slit interference experiment. *Phys. Rev. Lett.*, 73, 3149-3152 (1994).
  - [2] Yacoby, A., Heiblum, M., Mahalu, D. Shtrikman, H. Coherency and Phase sensitive measurements in a quantum dot. *Phys. Rev. Lett.*, 74, 4047-4050 (1994).
  - [3] Schuster, R. et al. Phase measurement in a quantum dot via a double-slit interference measurement. *Nature*, 385, 417-420 (1997).
  - [4] Ji, Y., Heiblum, M., Sprinzak, D., Mahalu, D. Shtrikman, H. Phase Evolution in a Kondo-correlated system. *Science*, 290, 779-783 (2000).
  - [5] Buks, E., Schuster, R., Heiblum, M., Mahalu, D. Shtrikman, H. Dephasing in electron interference by a 'which-path' detector. *Nature* 391, 871-820 (1998).
  - [6] van der Wiel, W. G. et al. The Kondo effect at unitary limit. *Science*, 289, 2105-2108 (1997).
  - [7] Buttiker, M. Four terminal phase coherent conductance. *Phys. Rev. Lett.*, 57, 1761-1764 (1986).
  - [8] Prange, R. E. Girvin, S. M. (Eds.) *The Quantum Hall Effect*, Springer, New York, 1987.
  - [9] Born, M. Wolf, E. *Principles of Optics*, 7th (expanded) version, Cambridge University Press, 1999, pp 348-352.
  - [10] Aharonov, Y. Bohm, D. Significance of electromagnetic potentials in the quantum theory. *Phys. Rev.* 115, 485-491 (1959).
  - [11] Aronov, A. G. Sharvin, Yu. V. Magnetic flux effects in disordered conductors. *Rev. Mod. Phys.* 59, 755-779 (1987).
  - [12] de-Picciotto, R. et al. Direct observation of a fractional charge. *Nature* 389, 162-165 (1997).

- [13] Reznikov, M. et al. Quantum shot noise. Superlattice and microstructures., 23, 901-915 (1998).
- [14] Chklovskii, D. B., Shklovskii, B. I., Glazman, L. I. Electrostatics of edge channels. Phys. Rev. B 46, 4026-4034 (1992).
- [15] Kane, C. L. Telegraph Noise and Fractional Statistics in the Quantum Hall Effect. cond-mat/0210621.